10th ANKARA INTERNATIONAL AEROSPACE CONFERENCE **AIAC-2019-090**
18-20 September 2019 - METU, Ankara TURKEY

AERODYNAMIC STABILITY ANALYSIS OF A FLAPPING WING IN HOVER USING STATE-SPACE REPRESENTATION

Ülgen Gülçat[1]
İTÜ
İstanbul

ABSTRACT

A fast method for determining the stability of a flapping wing Micro Air Vehicle (MAV) in hover is developed. The method is applied to determine the longitudinal stability of a flapping wing's aerodynamic force and moment, due to the pitch angle and its rate, coupled with the flight dynamics. The flight dynamic parameters interacting with the state-space representation of the aerodynamic loadings creates a matrix system expressed in stability derivatives and associated displacements and rates. This matrix system takes care of the simultaneous interaction of the longitudinal motion of the body with the state variables related to the pitching motion. The application here is made on the longitudinal stability of a fruit fly in hover. The results of the application shows that the trim with symmetric flapping is only possible with trivial solution. However, anti-symmetric flapping is suitable for trim. This result agrees with the findings in the related literature.

INTRODUCTION

The interest in the flapping wing MAVs has become quite intense because of less noise production and more efficient performances as opposed to the MAVs with fixed wings. The unsteady aerodynamic load predictions take considearbly long time using numeriacal and experimental techniques. On the other hand fast methods are preffered for the flight dynamics and control applications. In unsteady aerodynamic applications the state-space representations of aerdynamic loadings result in very fast predictions compared to conventional methods. The state variable is either chosen formally or it is based on a change of a phsical enttity like the separation point location on an airfoil [Goman and Khrabrov, 1994], [Gulcat, 2011 and 2016] and [Uhlig and Selig, 2017]. The timewise change of the state variable is given as the numerical solution of a first order ordinary differential equation. There are more complex applications, like spanwise morphing of a wing [Reich et.al., 2011] and [Izraelevitz et.al., 2017]. The formal approach employs the Duhamel integral together with the Wagner function [Taha et.al, 2014] and [Gulcat, 2017] or employs the Laplace transform [Leishman, 2000]. The Wagner function for a thin airfoil and for some elliptical wings with different aspect ratios are given in [Bisblinghoff, et.al, 1996].

In this study the Wagner function is employed to pedict the stability of a body whose wing is sweeping back and forth with varying angle of attack while hovering. The time lag between the wing motion and its aerodynamic response is given with the Wagner function. Here, because of sweeping motion the reduced speed changes periodically instead of being expressed with a constant free-stream speed. That is the reason for the exponents of the Wagner function

[1] Prof. Dr., Faculty of Aeronautics and Astronautics, e-mail: gulcat@itu.edu.tr

changes periodically with time. The aerodynamic loads due to wing flapping can be determined in a fast manner to interact with the equation of motion for the body.

The system of coupled eqations assuring the balance of aerodynamic loads with the the body motion, involving the stability derivatives, are formed to represent the small perturbations from the equilibrium. The conditions to satisfy the vanishing of these small perturbations for the hover and trim are given in [Taha et.al, 2014] and [Mouy et.al., 2017]. The application of the method on the trim of a fruit fly in hover is made satısfactorily with the pertinent data obatined from [Berman and Wang, 2007] and [Taha et.al, 2014], The resulting matrix system is 6x6 with time dependent quantities being the horizontal and vertical speeds, the pitch angle and its rate for the body and the pitch angle and its rate for the wing represented state-space. The resulting system for the flight dynamics coupled with the unsteady aerodynamic loads and its implementations will be provided in the method and the application section.

METHOD and APPLICATIONS

The lifting force and the moment for a thin airfoil undergoing arbitrary motion in a free stream U are given in [Bisblinghoff, et.al, 1996] with the Wagner function as follows

$$l(s)=\rho U^2 bC_l(s)=\rho b^2\pi(\ddot{h}+U\dot{\alpha})-2\rho U b\pi\left[w(b/2,s)\Phi(0)+\int_0^s w(b/2,\sigma)\frac{d\Phi(s-\sigma)}{d\sigma}d\sigma\right], \quad (1)$$

and

$$M(s)=\rho U^2 b^2 C_m(s)=-\frac{\rho b^3\pi}{2}(b\ddot{\alpha}/4+U\dot{\alpha})-\rho U b^2\pi\left[w(b/2,s)\Phi(0)+\int_0^s w(b/2,\sigma)\frac{d\Phi(s-\sigma)}{d\sigma}d\sigma\right] \quad (2)$$

Here, *b* is the half chord, *w(b/2,s)* is the downwash at three quarter chord and $\Phi(s)=1-a_1e^{-b_1 s}-a_2e^{-b_2 s}$ is the 2-D Wagner function. For the variable frue stream speed the reduced speed reads as $s=\frac{1}{b}\int_0^t U(\tau)d\tau$, and for the constant free stream *s=Ut/b.*

The equation of motion for the airfoil is $z_a(x,t)=-h(t)-\alpha(t)(x-a)$, and the associated downwash reads as

$$w(b/2,t)=\frac{\partial z_a}{\partial t}+U\frac{\partial z_a}{\partial x}=-\dot{h}(t)-\dot{\alpha}(t)\left[b/2-a\right]-U\alpha(t) \quad (3)$$

wherein, a is the pitch point location. Now, we can wtie the expression for the quasi-steady circulation as follows

$$\Gamma_{qs}(t)=bU(t)C_{ls}(\alpha(t))+\pi b(b/2-a)\dot{\alpha}(t)+\pi b\dot{h}(t) \quad (4)$$

Here, $C_{ls}=A\sin 2\alpha$, [Taha, et.al. 2014] is the sectional lift coefficient at high angles of attack including the effect of the leading edge vortex and it is the replacement for the convective term in (4). Comparing Equations (4) and (5) gives us the relation between the downwash and the circulation as follows

$$w(b/2,t)=-\Gamma_{qs}(t)/\pi b \quad (5)$$

If we substitute Equation (5) in (1) and (2) then the lift and the moment becomes

$$l(s)=\rho U^2 bC_l(s)=\rho\pi b^2(\ddot{h}+U\dot{\alpha})+2\rho U\left[\Gamma_{qs}(s)\Phi(0)+\int_0^s\Gamma_{qs}(s)\frac{d\Phi(s-\sigma)}{d\sigma}d\sigma\right] \quad (6)$$

and

$$M(s)=\rho U^2 b^2 C_m(s)=-\frac{\rho b^3\pi}{2}(b\ddot{\alpha}/4+U\dot{\alpha})+\rho U b\left[\Gamma_{qs}(s)\Phi(0)+\int_0^s\Gamma_{qs}(s)\frac{d\Phi(s-\sigma)}{d\sigma}d\sigma\right] \quad (7)$$

For the variable free stream the derivative of the Wagner function reads as

$$\frac{d\,\Phi(t-\tau)}{d\tau} = -a_i \frac{b_i}{b} U(\tau) e^{-\frac{b_i}{b}\int_{\tau}^{t} U(\varsigma)d\tau}, \quad i=1,2 \tag{8}$$

Then Equation (8) gives the time dependent circulation with

$$\Gamma_c(t) = (1-a_1-a_2)\Gamma_{qs}(t) + x_i(t) \tag{9}$$

And with

$$x_i(t) = \int_0^t \Gamma_{qs}(\tau)\, a_i \frac{b_i}{b} U(\tau) e^{-\frac{b_i}{b}\int_{\varsigma}^{t} U(\varsigma)d\tau} d\tau$$

Using the Leibnitz's rule for the derivation with respect to time makes Equation (8) to read

$$\dot{x}_i(t) = \frac{b_i}{b} U(t)\,(-x_i(t) + a_i\,\Gamma_{qs}(t)), \quad i = 1,2 \tag{10}$$

Here, $x_i=x_i(t)$ time dependent state variable which is responsible for the unsteady lift, and it is obtained as the solution of a first order ODE, Eqaution (10), with the initial condition of $x_i(0)=0$. Now, the circulatory unsteady lift becomes

$$l_c(t) = \rho U(\tau)\left[(1-a_1-a_2)\Gamma_{qs}(t) + x_1(t) + x_2(t)\right] \tag{11}$$

The non-circulatory lift on the other hand reads as

$$l_{nc}(t) = -\pi \rho b^2 a_z(t) \cos\eta(t) \tag{12}$$

Wherein , $a_z(t)$ is the vertical acceleration and $\eta(t)$ is the pitch angle. The acceleration is creared by: i) free stream speed change $-r\ddot{\varphi}\sin\eta$, and ii) angle of attack change $-r\dot{\varphi}\dot{\eta}\cos\eta$ make the total acceleration to become. From Equations (11) and (12) the total lift coefficient reads

$$C_l(t) = \frac{l_c(t) + l_{nc}(t)}{\rho U_m{}^2 b_m} \tag{13}$$

Here, U_m is the midspan maximum free stream speed, and b_m is half-chord at the midspan. The solution for a rectangular wing with certain aspect ratio is given in [Gulcat, 2017]. Here, the unsteady aerodynamic loads are going to be calcualted for a flappig elliptical wing of aspect ratio 3 as depicted in (Figure 1).

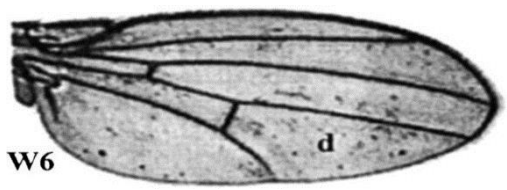

Figure 1: Wing of a f y. (Dimensions: body to root: 0.20mm, span: 2.02mm, mid-chord: 0.86mm, S=1.36mm^2)
(www.google.com.tr/search?q=shape+of+the+fruit+fly+wing)

Finite Wing:

The Wagner function for the elliptical wing of aspect ratio 3 is given as $\Phi_W(s) = 0.6 - 0.17e^{-o.54s}$ [Bisplinghoff, et al, 1996]. The sectional lift coefficients given with (11)

and (12) if integrated wirh respect to span give these values for the wing as follows

$$\int_{r_1}^{r_1+R}(l_c(t)+l_{nc}(t))dr=\rho\int_{r_1}^{r_1+R}\{U(\tau)\left[(0.6-0.17)\Gamma_{qs}(t)+x_1(t)+x_2(t)\right]-\pi\rho b^2 a_z(t)\cos\eta(t)\}dr \quad (14)$$

There are 3 resulting terms at the right hand side of (14) if we take $U(\tau)=\dot{\varphi}r$. These are: i) circulatory terms from the pitch and pitch rate, and ii) non circulatory term. Hence,

Pitch: $$l_{cp}(t)=\rho I_2\dot{\varphi}\left[0.43C_L(\alpha,t)+x_1(t)\right],\quad I_2=\int_{r_1}^{r_1+R}r^2 b\,dr$$

Pitch rate: $$l_{cpr}(t)=\rho I_1\dot{\varphi}\left[0.43\pi\dot{\alpha}(t)/2+x_2(t)\right],\quad I_1=\int_{r_1}^{r_1+R}rb^2dr$$

Here, $$\dot{x}_1(t)=\frac{b_1\bar{r}\dot{\varphi}(t)}{\bar{b}}\left[-x_1(t)+0.17\dot{\varphi}(t)C_L(\alpha,t)\right]\ \text{and}\ \dot{x}_2(t)=\frac{b_1\bar{r}\dot{\varphi}(t)}{\bar{b}}\left[-x_2(t)+0.17\dot{\alpha}(t)\right]$$

Non-circulatory: $$l_{nc}(t)=\pi\rho I_1\left[\ddot{\varphi}(t)\sin\eta(t)+\dot{\varphi}(t)\dot{\eta}(t)\cos\eta(t)\right]\cos\eta(t)$$

And $\bar{b}$ *and* $\bar{r}$ are the averaged half chord and half span and the static lift coefficient is $C_l=A\sin 2\alpha$, with A=1.833 [Taha et.al, 2014]. (Figure 2) shows the angle of attack change while the profile makes the sweeping motion.

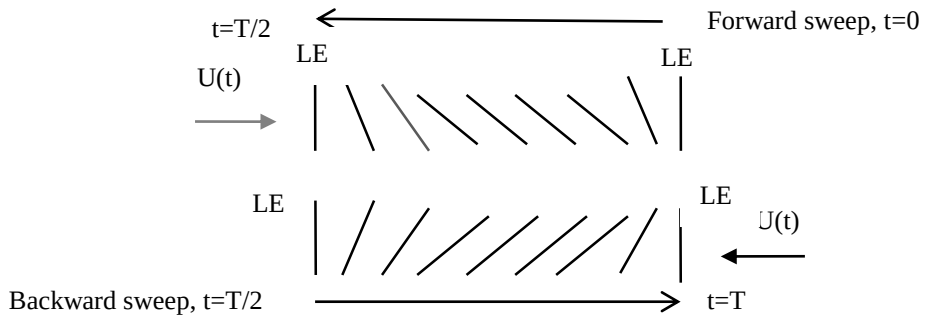

Figure 2: Angle of attack change during forward and backward sweep, 90º-40º-90º

Shown in (Figure 3) is the simplified wing-body cofiguration to represent the fruit fly. The coordinate axis shown are suitable for calculating the aerodynamic forces and moments.

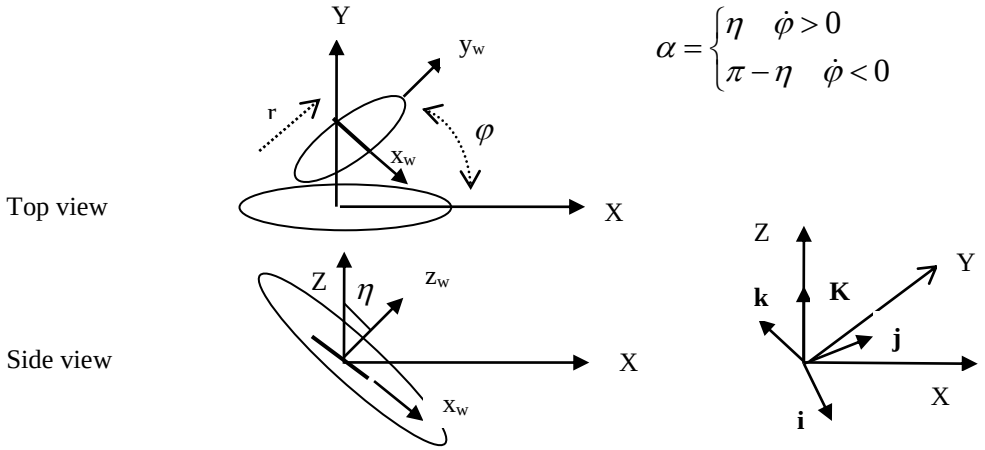

$$\alpha=\begin{cases}\eta & \dot{\varphi}>0\\ \pi-\eta & \dot{\varphi}<0\end{cases}$$

Figure 3: Wing-body configuration, top and side views

Appendix 1 provides the necessary information about the numerical values of I_1, I_2 and $\bar{b}$ to be used in the following equation

$$C_L(t) = \frac{l_{cr}(t) + l_{cp}(t) + l_{nc}(t)}{\rho U_m^2 S/2} \tag{15}$$

The variation of the total lift coefficient for one period is shown in (Figure 4) for the thin airfoil and for the wing.

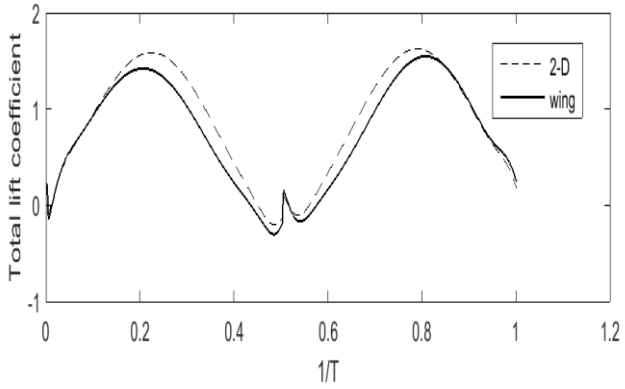

Figure 4: Variation of the total lift coefficient for a period.

Using (Figure 4) and Equation (15) for a period of the motion we get the result of the following integration as

$$\overline{C}_L = \frac{1}{T}\int_T^{2T} C_L(t)\,dt = 0.75 \tag{16}$$

Accordingly, the lifting force generated for both wings reads as

$$F = 2\overline{C}_L \rho U_m^2 S/2 = 7.11\mu N\,,$$

Here, the flapping frequency for the wing is *f=240 Hz* which is sufficient to lift the fruit fly which weighs about $W = 7.06\mu N$ [Berman and Wang, 2007].

The wing sweep here given by $\varphi = -75^o \cos\omega t$, and the change of the pitch angle is provided with the arctangent and sine functions as shown in (Figure 5). The free stream velocity span - wise variation is given by $\dot{\varphi} r = \overline{\varphi}\omega r \sin\omega t$.

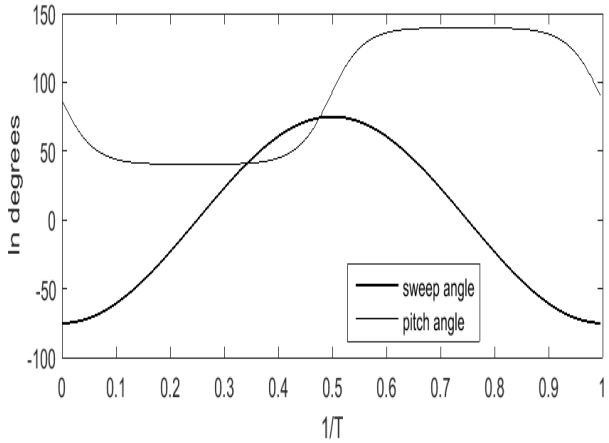

Figure 5: Sweep angle: $-75^o < \varphi < 75^o$, and the pitch angle, $40^o < \eta < 140^o$, variations.

Flight Stability

Study of the longitudinal stability of a body with a flapping wing requires the coupled treatment of unsteady aerodynamics with the parameters of the flight mechanics. Shown in (Figure 6)

are the necessary parameters to prescribe the hovering body under the gravity where the longitudinal and vertical velocity perturbation velocities are u and v respectively with also are the pitch rate of q and the pitch angle θ. The dynamic equilibrium equation using the notation of [Nelson,1998] reads as follows

$$\begin{pmatrix} \dot{u} \\ \dot{w} \\ \dot{q} \\ \dot{\theta} \end{pmatrix} = \begin{pmatrix} -qw - g\sin\theta \\ qu + g\cos\theta \\ 0 \\ q \end{pmatrix} + \begin{pmatrix} X/m \\ Z/m \\ M/I_y \\ 0 \end{pmatrix} \tag{17}$$

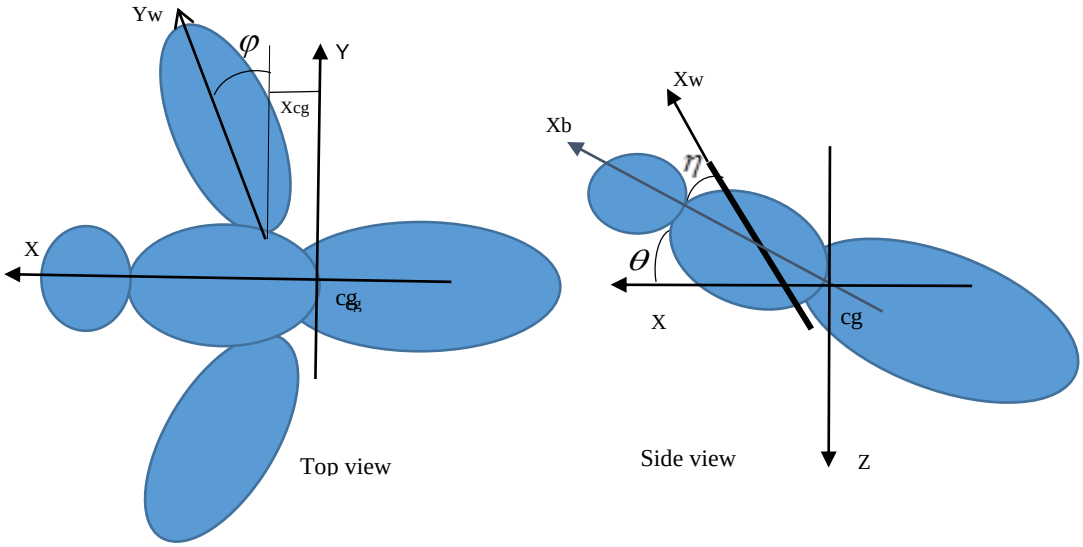

Figure 6: Reference frame and the parameters used for the flight stability.

Here, X, Z and M are the horizontal and the vertical forces and the pitching moment respectively, and m is the mass, I_y is the rotational moment of inertia and finally g is the gravitational acceleration.

Unsteady aerodynamics of a flapping wing gives the lift, moment in terms of the pitch and the pitch rate. Here, we implement the state varibles concept, x_1 and x_2 , with two ordinary differential equations in time involving the pitch and its rate:

$$\dot{x}_1(t) = \frac{b_1 U_{ref}}{\bar{b}}\left[-x_1(t) + a_1\dot{\varphi}(t)C_L(\alpha,t)\right] \text{ and } \dot{x}_2(t) = \frac{b_1 U_{ref}}{\bar{b}}\left[-x_2(t) + a_1\dot{\alpha}(t)\right]$$

If we let the sate variables interact with the equation of motion, (17), the perturbation equations for the system involves the rate of 6 variables , $\dot{\chi} = \left(\dot{u}\ \dot{w}\ \dot{q}\ \dot{\theta}\ \dot{x}_1\ \dot{x}_2\right)^T$, and their stability derivative matrix as follows

$$\begin{pmatrix} \dot{u} \\ \dot{w} \\ \dot{q} \\ \dot{\theta} \\ \dot{x}_1 \\ \dot{x}_2 \end{pmatrix} = \begin{pmatrix} -qw - g\sin\theta \\ qu + g\cos\theta \\ 0 \\ q \\ 0 \\ 0 \end{pmatrix} + \begin{pmatrix} X_0 \\ Z_0 \\ M_0 \\ 0 \\ X_{1_0} \\ 0 \end{pmatrix} + \begin{bmatrix} X_u & X_w & X_q & 0 & X_{x_1} & X_{x_2} \\ Z_u & Z_w & Z_q & 0 & Z_{x_1} & Z_{x_2} \\ M_u & M_w & M_q & 0 & M_{x_1} & M_{x_2} \\ 0 & 0 & 0 & 0 & 0 & 0 \\ X_{1_u} & X_{1_w} & X_{1_q} & 0 & X_{1_{x_1}} & 0 \\ 0 & 0 & X_{2_q} & 0 & 0 & X_{2_{x_2}} \end{bmatrix} \begin{pmatrix} u \\ w \\ q \\ 0 \\ x_1 \\ x_2 \end{pmatrix} \tag{18}$$

In Equation (18), the column vector expressed with subscript o shows the effect of pitch rate and the subscript for the coefficient matrix indicates the derivatives (Appendix 2). The horizontal sectional force is shown by, X' , and the vertical sectional force by, Z'. The sectional lift *l* and the drag *d* are employed to give these horizontal and vertical forces as follows

$$X' = -\mathrm{sgn}(\dot{\varphi})(d - l\alpha_i) \;\; and \;\; Z' = -(l + d\alpha_i)\,,\;\; \alpha_i \, induced \;\; angle \; of \; attack \qquad (19a,b)$$

Here, two differen contributions to the sectional forces are possible: i) from pitching l_P , ii) from pitch rate l_{Pr}, which are determined with x_1 and x_2 . On the other hand the induced angle of attack is small and can be approximated as

$$\alpha_i \cong \frac{w_{eff}}{|U|}, \quad and \quad w_{eff} = w - q(r\sin\varphi + a), \quad U \cong r\dot{\varphi} + u\cos\varphi$$

The perturbation velocities *u, w* and the pitch rate *q,* all contribute to the sectional lift coefficient in terms of pitch and the pitch rate. Considering the effective free stream velocities, the sectional lift forces read as

$$l_P = \rho(r\dot{\varphi} + u\cos\varphi)\mathrm{sgn}(\dot{\varphi})\left[b(r\dot{\varphi} + u\cos\varphi)A(\sin 2\eta + 2\alpha_i\cos 2\eta)\Phi(0) + x_1(t)\right], \text{ and}$$

$$l_{\mathrm{Pr}} = \rho(r\dot{\varphi} + u\cos\varphi)\mathrm{sgn}(\dot{\varphi})\pi b^2\left[q\cos\varphi + (1/2 - a)q\cos\varphi\,\Phi(0) + x_2(t)\right] \qquad (20a,b)$$

Similarly, the sectional drag becomes

$$d_P = \rho(r\dot{\varphi} + u\cos\varphi)\mathrm{sgn}(\dot{\varphi})\left[b(r\dot{\varphi} + u\cos\varphi)A(\sin^2\eta + \alpha_i\sin 2\eta)\Phi(0) + x_1(t)\right]$$

Since the induced angle of attack is small the second order terms are neglected, and this gives the induced lift and the drag as follows

$$l_P\alpha_i = \rho\, w_{eff}\left[brA\dot{\varphi}\sin 2\eta\,\Phi(0)\right], \qquad d_P\alpha_i = \rho\, w_{eff}\left[2brA\dot{\varphi}\sin^2\eta\,\Phi(0)\right] \qquad (21a,b)$$

Averaging

Equation (18) is now utilized for the stability analysis of the time dependent periodic system. For this purpose, we take the time average of the quantities for a period of time T as

$$\dot{\bar{\chi}} = f(\bar{\chi}) + h(\bar{\chi}), \;\; here \;\; h(\bar{\chi}) = \frac{1}{T}\int_0^T h(\chi, t)dt$$

Now, the averaged sysytem reads as

$$\begin{pmatrix} \dot{\bar{u}} \\ \dot{\bar{w}} \\ \dot{\bar{q}} \\ \dot{\bar{\theta}} \\ \Delta\dot{\bar{x}}_1 \\ \dot{\bar{x}}_2 \end{pmatrix} = \begin{pmatrix} -\bar{q}\bar{w} - g\sin\bar{\theta} \\ \bar{q}\bar{u} + g\cos\bar{\theta} \\ 0 \\ 0 \\ 0 \\ 0 \end{pmatrix} + \begin{pmatrix} \bar{X}_0 + \bar{X}_{x_1}\bar{x}_{1eq} \\ \bar{Z}_0 + \bar{Z}_{x_1}\bar{x}_{1eq} \\ \bar{M}_0 + \bar{M}_{x_1}\bar{x}_{1eq} \\ 0 \\ 0 \\ 0 \end{pmatrix} + \begin{bmatrix} \bar{X}_u & \bar{X}_w & \bar{X}_q & 0 & \bar{X}_{x_1} & \bar{X}_{x_2} \\ \bar{Z}_u & \bar{Z}_w & \bar{Z}_q & 0 & \bar{Z}_{x_1} & \bar{Z}_{x_2} \\ \bar{M}_u & \bar{M}_w & \bar{M}_q & 0 & \bar{M}_{x_1} & \bar{M}_{x_2} \\ 0 & 0 & 1 & 0 & 0 & 0 \\ \bar{X}_{1_u} & \bar{X}_{1_w} & \bar{X}_{1_q} & 0 & \bar{X}_{1_{x_1}} & 0 \\ 0 & 0 & \bar{X}_{2_q} & 0 & 0 & \bar{X}_{2_{x_2}} \end{bmatrix} \begin{pmatrix} \bar{u} \\ \bar{w} \\ \bar{q} \\ \bar{\theta} \\ \Delta\bar{x}_1 \\ \bar{x}_2 \end{pmatrix} \qquad (22)$$

Here, $\Delta\dot{\bar{x}}_1 = \dot{\bar{x}}_1 - \dot{\bar{x}}_{1eq}$ *and* $\bar{x}_{1eq} = -\bar{X}_{1_0} / \bar{X}_{1_{x1}}$. The algebraic Equations (22) are solved for $\left(\bar{u} = 0,\, \bar{w} = 0,\; \bar{q} = 0,\;\; \bar{\theta} = 0\right)$ in hover.

Trim in hover

The time averaged equation of motion is now implemented for the trimming of the hovering body while flapping its wings. For the wing flapping, thereare two different types; İ) symmetric flapping, and ii) anti-symmetric flapping.

i) Trim with symmetric flapping

For the sake of smplicity, we choose the time dependent sweeping motion as a saw-tooth shaped which is expressed as (Mouy, 2017)

$$\varphi(t)=\begin{cases} 4\bar{\varphi}/T(t-T/4), & 0\le t\le T/2 \\ -4\bar{\varphi}/T(t-3T/4), & T/2\le t\le T \end{cases}$$

During the sweeping motion of the wing, a piecewise constant angle of attack is considered as follows

$$\eta(t)=\begin{cases} \bar{\alpha}, & 0\le t\le T/2 \\ \pi-\bar{\alpha}, & T/2\le t\le T \end{cases}$$

During the symmetric sweeping, the full unsteady treatment gives a non-zero value for the X force component, whereas the quasi-steday approach yields 0 result (Mouy, et.al., 2017). The full unsteady treatment results in Equation (22) for the x direction, in terms of averaged values, as follows (Appendix3):

$$\bar{X}_{x_1}\bar{x}_{1eq}=8\frac{\rho I_{10}}{mT^2}\bar{r}2\bar{b}\,\bar{\varphi}\sin\bar{\varphi}Aa_1\sin 2\bar{\alpha} \tag{23}$$

The right hand side of Equation (23) is 0 only for the average sweep or the angle of attack, $\bar{\varphi}=0$ *or* $\bar{\alpha}=0$. This means trimming is possible only for the no sweep or no lift! For this reason we have to resort to antisymmetric sweep.

ii) Trim with anti-symmetric flapping
In order to achieve trim during hover the sweeping motion is modified as follows :

$$\varphi(t)=\begin{cases} \bar{\varphi}_0+4\bar{\varphi}/T(t-T/4), & 0\le t\le T/2 \\ \bar{\varphi}_0-4\bar{\varphi}/T(t-3T/4), & T/2\le t\le T \end{cases}$$

The angle of attack:

$$\eta(t)=\begin{cases} \bar{\alpha}_d, & 0\le t\le T/2 \\ \pi-\bar{\alpha}_u, & T/2\le t\le T \end{cases}$$

The trim equations then read:

$$\begin{aligned} &\bar{X}_0+\bar{X}_{x1}\bar{X}_{1eq}=0 \\ &\bar{Z}_0+\bar{Z}_{x1}\bar{X}_{1eq}=-g \\ &\bar{M}_0+\bar{M}_{x1}\bar{X}_{1eq}=0 \end{aligned} \tag{24a,b,c}$$

In Equation (24), there are 3 equations and 3 unknowns; $\bar{\alpha}_d$, $\bar{\alpha}_u$ *and* $\bar{\varphi}_0$. We use the time averaged values for the stability dervatives to obtain following non-linear expressions (Appendix 3).

Force balance in X: $$\sin 2\bar{\alpha}_d+\sin 2\bar{\alpha}_u=-\frac{I_{21}}{I_{10}\bar{r}\bar{b}}(\sin^2\bar{\alpha}_d-\sin^2\bar{\alpha}_u)(0.6-a_1)/a_1 \tag{25}$$

Force balance in Z: $$\sin 2\bar{\alpha}_d+\sin 2\bar{\alpha}_u=\frac{mgT^2}{4\rho A(0.43I_{21}+0.17I_{10}\bar{r}2\bar{b})\bar{\varphi}^2} \tag{26}$$

Moment balance in M:

$$a\sin\bar{\varphi}\cos\bar{\varphi}\left[0.43I_{22}(\sin\bar{\alpha}_d-\sin\bar{\alpha}_u)-0.17I_{11}\bar{r}2\bar{b}(\sin 2\bar{\alpha}_d+\sin 2\bar{\alpha}_u)\right]x$$
$$(\cos\bar{\alpha}_d+\sin\bar{\alpha}_d-\cos\bar{\alpha}_u+\sin\bar{\alpha}_u)+0.43x_{cg}\bar{\varphi}(\sin 2\bar{\alpha}_d+\sin 2\bar{\alpha}_u)(I_{21}-2I_{10}\bar{r}2\bar{b}) \quad (27)$$
$$+\sin\bar{\varphi}(0.43I_{31}\cos\bar{\varphi}_0-0.17I_{20}4\bar{r}\bar{b}\sin\bar{\varphi}_0)(\sin 2\bar{\alpha}_d+\sin 2\bar{\alpha}_u)=0$$

Here, a is distance between the pitch point and the quarter chord.

We solve for X and Z force balances (25) and (26) , to obtain $\bar{\alpha}_d$ *and* $\bar{\alpha}_u$ in terms of the sweep angle and the period, $\bar{\varphi}$ *and* T , respectively. Hence, we can calculate the angle of attack for the forward and backward sweeps. Afterwards, by the aid of (27) the initial sweep angle $\bar{\varphi}_0$ is determined to complete the solution for the trim in hover.

Trimming of fruit-fly in hover:

The pertinent parameters for a fruit-fly is provided as follows [Berman and Wang, 2007) :

m=0.72mg, f=254Hz, $\bar{\varphi}=75^0$, a=0, x_{cg}=0.5, I_{10}=4.89, I_{11}=3.30, I_{21}=4.69, I_{20}=7.29, I_{22}=3.32, I_{31}=7.36

From the simultaneous solution of (25), (26) and (27), the anti-symmetric trim results are obtained as follows

$\bar{\alpha}_d$ = 34.3^0, $\bar{\alpha}_u$ = 55.6^0 and $\bar{\varphi}_0$ = 4^0

For this case the angle of attack differs for the forward and the backward sweeps. The angle of attack becomes 34.3^0 for the forward sweep and 55.6^0 in backward sweep. During sweeping the forward sweep angle changes -71^0< $\varphi(t)$ <79^0 and in backward sweep 79^0> $\varphi(t)$ > -71^0. The time change of sweep and angles of attack are given for both symmetric and antisymmetric cases in (Figure 7). The deviation from the symmetric case is about 5^0 for the angle of attack and 4^0 for the sweep, which can be applied easily for the control purposes.

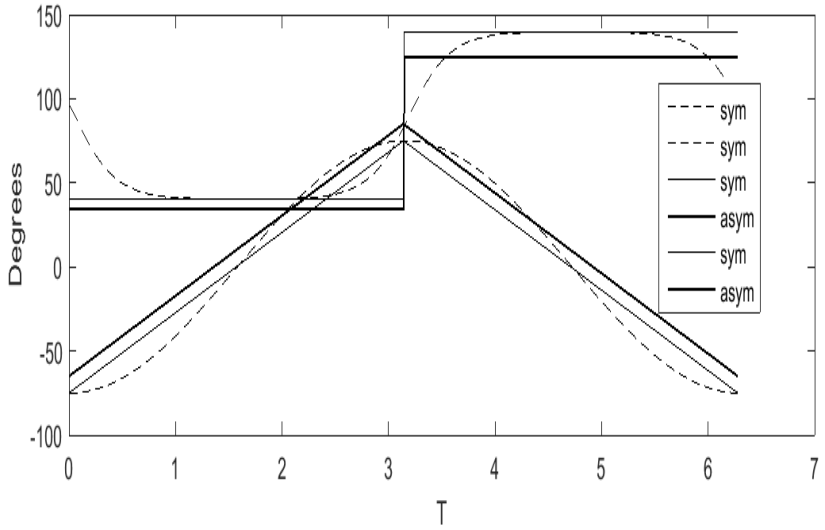

Figure 7: Trimmed antisymmetric sweep and angle of attack____, un-trimmable symmetric sweep -----.

CONCLUSION

The state space approach is satisfactorily implemented for the hovering body whose wings are flapping with forward and backward sweep for generation of unsteady aerodynamic forces and moments.

In order to maintain hover the necesary conditions are expressed in terms of the small perturbation values related to the stability derivatives. These quantities are timewise periodic therefore, time averaged values are used for determining the stability of hovering.

Utilizing the time averaged full unsteady values trimmig of the hover was possible for the antisymmetric flapping. Via symmetric flapping full unsteady treatment does not allow triim conditions to apply. On the other hand, the symmetric flapping with quasi steady treatment allows trimming while neglecting the full unsteadiness of the flow.

Appendices

App1: The properties of the eliptical wing shape of the fruit fly is given in Figure A. Accordingly, the first and the second moment of inertia for the wing read as

$$I_1/2 = \int_{r_1}^{r_1+R} r b^2(r)dr$$ =eval(int((-(x-1.01-.20)^2/1.01^2+1)*0.43^2*x,.20,2.22))= 0.3013 mm^4

$$I_2/2 = \int_{r_1}^{r_1+R} r^2 b(r)dr$$ =eval(int(sqrt(-(x-1.01-.20)^2/1.01^2+1)*0.43^2*x^2,.20,2.22)=0.5043 mm^4

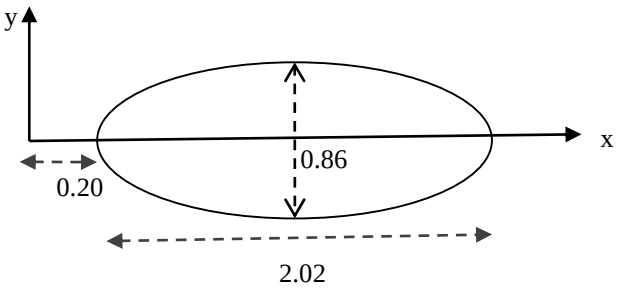

r_1=0.20
R=2.02
$\bar{r}$ =1.21
b=0.43
S=1.36mm^2
AR=3

Figure A. Pertinent dimensions, in mm, of the elliptical wing of a fruit fly.

The equation of the ellipse is $$\frac{(r-1.01-0.20)^2}{(1.01)^2}+\frac{b^2}{(0.43)^2}=1$$

App2: Aerodynamic forces and moments at a constant AoA.

$$K_{mn}=\rho A I_{mn}/2,\quad I_{mn}=2\int_{r_1}^{R} r^m c^n(r)dr,\quad I_y = Moment\ of\ inertia\ \ of\ the\ body$$

$$X_{P0}=-2\frac{K_{21}}{m}\dot{\varphi}|\dot{\varphi}|\cos\varphi\sin^2\eta\,\Phi(0)\qquad Z_{P0}=-\frac{K_{21}}{m}\dot{\varphi}|\dot{\varphi}|\sin 2\eta\,\Phi(0)$$

$$M_{P0}=2|\dot{\varphi}|\dot{\varphi}\sin\eta\left(\frac{K_{21}}{I_y}x_{cg}\cos\eta+\frac{K_{22}}{I_y}a\cos\varphi+\frac{K_{31}}{I_y}\sin\varphi\cos\eta\right)\Phi(0).$$

Partial derivatives of forces and moments:

x-dir:

$$X_{Pu}=-4\frac{K_{11}}{m}|\dot{\varphi}|\cos^2\varphi\sin^2\eta\,\Phi(0),\qquad X_{Pw}=-\frac{K_{11}}{m}|\dot{\varphi}|\cos\varphi\sin 2\eta\,\Phi(0),$$

$$X_{Pq}=\left(\frac{K_{21}}{m}|\dot{\varphi}|\cos\varphi\sin\varphi\sin 2\eta+x_{cg}\frac{K_{11}}{m}|\dot{\varphi}|\cos\varphi\sin 2\eta\right)\Phi(0),\ X_{Px_1}=-\rho\frac{I_{10}}{m}|\dot{\varphi}|\cos\varphi\ ,\ X_{Px_2}=0.$$

z-dir;

$$Z_{Pu} = -4\frac{K_{11}}{m}|\dot{\varphi}|\cos^2\varphi\,\Phi(0), \quad Z_{Pw} = Z_{Pu}/2, \quad Z_{Pq} = \frac{K_{21}}{m}|\dot{\varphi}|\sin\varphi\sin^2\eta\,\Phi(0) - x_{cg}Z_{Pw},$$

$$Z_{Px_1} = -\rho\frac{I_{10}}{m}|\dot{\varphi}|, \quad Z_{Px_2} = 0.$$

Moments:

$$M_{Pu} = 4\frac{K_{12}}{I_y}a|\dot{\varphi}|\cos^2\varphi\sin\eta\,\Phi(0) + 2\frac{m}{I_y}X_{Pq},$$

$$M_{Pw} = 2(\frac{K_{12}}{I_y}a|\dot{\varphi}|\cos\varphi\cos\eta + \frac{K_{21}}{I_y}a|\dot{\varphi}|\cos\varphi\cos^2\eta)\Phi(0) - \frac{m}{I_y}x_{cg}Z_{Pw}$$

$$M_{Pq} = 2|\dot{\varphi}|(a\cos\varphi\cos\eta(\frac{K_{12}}{I_y}x_{cg} + \frac{K_{22}}{I_y}\sin\varphi) - \sin\varphi\cos^2\eta)(\frac{K_{21}}{I_y}x_{cg} + \frac{K_{31}}{I_y}\sin\varphi))\Phi(0) - \frac{m}{I_y}x_{cg}Z_{Pq}$$

$$M_{Px_1} = \rho\frac{I_{11}}{I_y}a|\dot{\varphi}|\cos\varphi(\cos\eta + \sin\eta) + \rho\frac{I_{20}}{I_y}|\dot{\varphi}|\sin\varphi\cos^2\eta - \frac{m}{I_y}x_{cg}Z_{Px_1}, \quad M_{P_2} = 0$$

Partial derivatives of aerodynamic forces and moments wrt pitch rate i:

x-dir: 0 contribution to the derivatives of X.

z-dir:

$$Z_{\mathrm{Pr}q} = -\frac{K_{\mathrm{Pr}_{12}}}{m}\dot{\varphi}\cos\varphi\,\Phi(0) - \rho\frac{I_{12}}{m}\pi\dot{\varphi}\cos\varphi \qquad Z_{\mathrm{Pr}_{x_2}} = -\rho\frac{I_{21}}{m}\dot{\varphi}\ , \quad K_{\mathrm{Pr}_{mn}} = \pi\rho(1/2-a)I_{mn}$$

Rest of the derivatives of Z is 0.

Moment:

$$M_{\mathrm{Pr}q} = \dot{\varphi}\cos\varphi(\frac{K_{\mathrm{Pr}13}}{I_y}a\cos\varphi\cos\eta + \frac{K_{\mathrm{Pr}22}}{I_y}\sin\varphi)\Phi(0) - \rho\pi\frac{I_{13}}{I_y}\dot{\varphi}\cos\varphi - \frac{K_v}{I_y}\mu\, f\cos^2\varphi, \quad K_v = \frac{\pi}{16}\rho I_{04}$$

$$M_{\mathrm{Pr}x_2} = \rho\frac{I_{11}}{I_y}a|\dot{\varphi}|\cos\varphi(\cos\eta + \sin\eta) + \rho\frac{I_{20}}{I_y}|\dot{\varphi}|\sin\varphi - \frac{m}{I_y}x_{cg}Z_{\mathrm{Pr}x_2}$$

Pitch derivatives:

$$X_{1_u} = 2b_1\bar{r}|\dot{\varphi}|Aa_1\sin2\eta\cos\varphi, \qquad X_{1_w} = 2b_1\bar{r}|\dot{\varphi}|\dot{\varphi}Aa_1\cos2\eta\ ,$$
$$X_{1q} = -2b_1\bar{r}|\dot{\varphi}|Aa_1(x_{cg} + \bar{r}\sin\varphi)\ , \quad X_{1_{x1}} = -b_1\bar{r}|\dot{\varphi}|/b$$

Last 2 derivatives realted to pitch:

$$X_{2_q} = 2b_1\bar{r}|\dot{\varphi}|\pi(b/2-a)a_1\cos\varphi + b_1\bar{r}|\dot{\varphi}|\pi\, a_1\cos\varphi, \quad X_{2_{x2}} = -b_1\bar{r}|\dot{\varphi}|/b$$

App3: Trim Parameters:

i) Symmetric:

$$\overline{X}_{x1} = -\frac{1}{T}\int_0^T \rho\frac{I_{10}}{m}|\dot{\varphi}|\cos\varphi\,dt = \rho\frac{I_{10}}{m}\frac{1}{T}\frac{4\overline{\varphi}}{T}\left[\int_0^{T/2}\cos\frac{4\overline{\varphi}}{T}(t - T/4)\,dt + \int_{T/2}^{T}\cos\frac{4\overline{\varphi}}{T}(t - 3T/4)\,dt\right]$$

$$= -\rho\frac{I_{10}}{m}\frac{1}{T}\left[\sin\frac{4\overline{\varphi}}{T}(t - T/4)\Big|_0^{T/2} + \sin\frac{4\overline{\varphi}}{T}(t - 3T/4)\Big|_{T/2}^{T}\right] = \rho\frac{I_{10}}{m}\frac{1}{T}(\sin\overline{\varphi} + \sin\overline{\varphi} + \sin\overline{\varphi} + \sin\overline{\varphi})$$

$$= 4\rho\frac{I_{10}}{mT}\sin\overline{\varphi}$$

$$\overline{X}_{1eq}=\frac{\overline{X}_{10}}{\overline{X}_{1x_1}}=\frac{\frac{1}{T}\int_0^T b_1\bar{r}^2|\dot{\varphi}|\dot{\varphi}\,Aa_i\sin 2\eta\,dt}{-2b_i\bar{r}|\dot{\varphi}|/\bar{c}}=\frac{Aa_1}{2T}(\int_0^{T/2}\dot{\varphi}\sin 2\overline{\alpha}dt+\int_{T/2}^{T}\dot{\varphi}\sin 2(\pi-\overline{\alpha})dt)$$

$$=\frac{Aa_1}{2T}(\frac{4\overline{\varphi}}{T}\sin 2\overline{\alpha}\,t\Big|_0^{T/2}-\frac{4\overline{\varphi}}{T}\sin(-2\overline{\alpha}\,t)\Big|_{T/2}^{T})=\frac{2}{T}\overline{\varphi}Aa_1\sin 2\overline{\alpha}$$

After summing up we obtain (23).

$$\overline{X}_{x1}\overline{X}_{1eq}=8\rho\bar{r}2\bar{b}\,\frac{I_{10}}{mT^2}\overline{\varphi}\sin\overline{\varphi}Aa_1\sin 2\overline{\alpha}$$

ii) Antisymmetric: Integrating for a period:

Equation (24a)

$$\overline{X}_{P0}=-16\,\frac{\rho AI_{21}}{mT^2}\overline{\varphi}\cos\overline{\varphi}\sin\overline{\varphi}(\sin^2\overline{\alpha}_d-\sin^2\overline{\alpha}_u)\Phi(0)/2$$

and

$$\overline{X}_{x1}\overline{X}_{1eq}=8\rho\bar{r}2\bar{b}\,\frac{I_{10}}{mT^2}\overline{\varphi}\sin\overline{\varphi}\cos\overline{\varphi}Aa_1(\sin 2\overline{\alpha}_d-\sin 2\overline{\alpha}_u)$$

$\overline{X}_{P0}+\overline{X}_{x1}\overline{X}_{1eq}=0$ gives (24a), and (24b,c) are obtained similarly.

References

Berman, G.J. and Wang, Z.J. (2007) *Energy-minimazing kinematics in hovering flight*, J. Fluid Mech. Vol.582 p. 153-168.

Bisplinghoff, R.L., Ashley, H., Halfman, R.L. (1996) Aeroelasticity, Dover Publications Inc., New York, p. 393-394

Goman, M. and Khrabrov,A. (1994) *State-Space Representation of Aerodynamic Characteristics of an Aircraft in High Angles of Attack,* Jornal of Aircraft, Vol. 31, No. 5, p.1109-1115.

Gulcat, U. (2011) *Shortcuts in Unsteady and Flapping Wing Aerodynamics*, Invited Lecture, AIAC'2011-002, Sept.14-16 2011, METU, Ankara, TURKEY.

Gulcat, U. (2016) *Fundamentals of Modern Unsteady Aerodynamics*, 2nd Ed., Springer, p. 331-334.

Gulcat, U. (2017) *State-Space Representation of Flapping Wings in Hover,* 9th Ankara International Aerospace Conference, 20-22 Sept. 2017-METU, Ankara TURKEY, AIAC-2017-60.

Izraelevitz, J.S., Quiang, Z. And Triantafyllou, M.S. (2017) *State-Space Adaptation of Unsteady Lifting Line Theory Twisting/Flapping Wings of Finite Span,* AIAA Journal, Vol. 55, No. 4, p. 1279-1294.

Leishman, G. (2000) *Principle of Helicopter Aerodynamics,* Cambridge University Press, p. 341-342.

Mouy, A., Rossi, A. And Taha, H.E. (2017) *Coupled Unsteady Aero-Flight Dynamics of Hovering Insects/Flapping Micro Air Vehicles,* Journal of Aircraft, Vol. 54, No. 5, p. 1738-1749.

Nelson, R.C. (1998) *Flight Stability and Automatic Control,* Vol. 2, McGraw-Hill, New York, p. 217.

Reich, G.W., Eastep, F.E., Altman, A. and Alberani, R. (2011) *Transient Poststall Aerodynamic Modeling for Extreme Maneuvers in Micro Air Vehicles,* Journal of Aircraft, Vol.48, No. 2, p.403-411,

Taha, H.E., Hajj, M.R. and Beran, P.S. (2014) *State-Space Representation of the Unsteady Aerodynamics of Flapping Flight*, Aerospace Science and Technology, Vol. 34, p.1-11.

Taha, H.E., Hajj, M.R. and Nayfeh, A.H. (2014) *Longitudinal Flight Dynamics Hovering MAVs/Insects,* Journal of Guidence, Control, and Dynamics, Vol. 37, No. 3, p, 970-978.

Uhlig, D.V. and Selig,M.S., 2017. *Modeling Micro Air Vehicle Aerodynamics in Unsteady High Angle of Attack Flight,* Journal of Aircraft, Vol. 54, No. 3, p. 1064-1075.